# Theory of a grating coupler of finite thickness

Lian Zheng and W. L. Schaich
*Department of Physics and Materials Research Institute, Indiana University, Bloomington, Indiana*
(Received 6 August 1990; revised manuscript received 15 October 1990)

We derive and evaluate expressions for the evanescent infrared fields near a grating coupler of finite thickness. The calculations confirm over a range of small thicknesses the validity of models used earlier in which the grating coupler was viewed as an inhomogeneously conducting sheet of negligible thickness. For thicker gratings the deviations from the simpler theories are evident, and their influence on the coupling to a two-dimensional electron gas are illustrated. Special care is necessary to ensure the numerical stability of the results.

A common way to study the excitations of electron systems with reduced dimensionality is with infrared absorption and often a grating coupler is used to allow additional momentum transfers parallel to the surface.[1-3] These gratings are physically separated from the system to be studied and the coupling occurs through the local fields generated in the grating. In an earlier paper,[4] we presented a theory of the optics of such systems that treated the grating as an idealized two-dimensional (2D) layer, which greatly simplified the calculations. Here we derive a three-dimensional (3D) description of a transmission grating coupler. Our aim is both to justify the 2D approximation for small thickness of the gratings and to develop an approach that can be used to quantify the corrections for larger thicknesses.

The specific system we study is shown in Fig. 1. The grating consists of a planar array of alternating rectangular bars of uniform conductors. The $\sigma$'s describe the conductance per square of each bar for current flowing in the $y$ direction. They are the same quantities that appear in the 2D approximation.[4] The (isotropic) 3D conductivities of the bars are described by $\sigma/D$, where $D$ is the grating thickness, and our focus is on how results depend on $D$ for fixed $\sigma$'s. This point of view is similar to that of Petit and Tayeb.[5] We assume the incident light is along

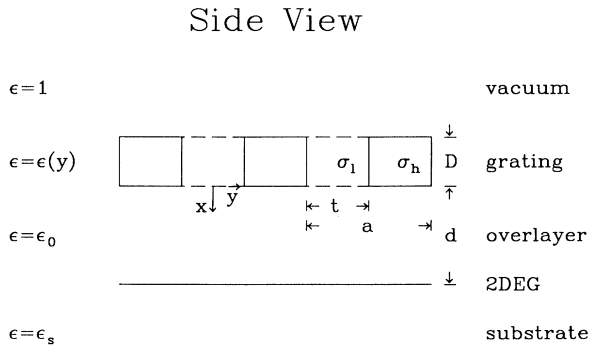


FIG. 1. Qualitative sketch of interface region showing how various parameters in the text are defined. Everything extends unchanged in the $z$ direction and has a period $a$ in the $y$ direction.

the normal $\hat{\mathbf{x}}$, coming from the vacuum above the system. It will interact with both the grating and the 2D electron gas (2DEG) embedded in the substrate below and we seek the net transmission. The physical separation of the grating and the 2DEG allows us to analyze their individual electrodynamic behavior separately and then to determine their coupled response by a multiple scattering scheme.

We begin with the behavior of the isolated grating and are immediately faced with many possible theoretical approaches.[6,7] Since our goal here is merely to determine the limit of validity of an earlier approximation to a specific problem, we follow a single approach which is readily adapted to that case. The analysis is based on the method of Sheng, Stepleman, and Sanda[8] and its key is an analytic determination of the eigenfunctions of Maxwell's equations in separate regions of space. The complete solution is expanded in such basis sets and the unknown coefficients are determined by matching across boundaries. Outside the grating the eigenfunctions are simple transverse plane waves, but inside their form is less obvious. However, our particular grating geometry allows a straightforward calculation.

We momentarily ignore the finite extent of the grating along $\hat{\mathbf{x}}$ and view it as a stack of infinite planar slabs alternating along $\hat{\mathbf{y}}$. The two types of slabs are characterized by the isotropic, complex-valued, dielectric functions $\epsilon_h, \epsilon_l$ derived from the high and low values of $\sigma$:

$$\epsilon_h = 1 + \frac{4\pi i \sigma_h}{\omega D}, \quad \epsilon_l = 1 + \frac{4\pi i \sigma_l}{\omega D} , \tag{1}$$

where $\omega$ is the light frequency. We consider only $H$-polarized solutions moving along $\hat{\mathbf{x}}$ for which the magnetic field appears as $\mathbf{H} = \hat{\mathbf{z}} H(x,y)$ with

$$H(x,y) = h(y)\exp(\pm\gamma x) . \tag{2}$$

The corresponding electric field $\mathbf{E}$ follows from Ampère's law

$$-i\frac{\omega}{c}\epsilon(y)\mathbf{E} = \nabla \times \mathbf{H} , \tag{3}$$

where $\epsilon(y)$ jumps between $\epsilon_h$ and $\epsilon_l$ with period $a$. We do not consider the alternate case of $E$ polarization since

 

for typical parameters the gratings of interest are efficient polarizers[4] and transmit negligible amounts of such fields, independent of whether they are treated as 2D or 3D entities. In the same spirit the experimental geometry allows us to look only for $h(y)$ functions in (2) that are periodic in $y$ (with period $a$) and even functions of both $y$ and $y-a/2$.

From Maxwell's equations the differential equation for $h(y)$ is

$$\frac{d^2h}{dy^2}+[\gamma^2+k_0^2\epsilon(y)]h=0\ , \tag{4}$$

where $k_0=\omega/c$. With our symmetry constraints we can write the relevant (non-normalized) solutions as

$$h(y)=\begin{cases}\cos\alpha_l y, & 0\le|y|\le t/2\\ A\cos\alpha_h\left[y-\dfrac{a}{2}\right], & 0\le|y-a/2|\le(a-t)/2\end{cases} \tag{5}$$

plus periodic extensions where

$$\alpha_l^2=\gamma^2+k_0^2\epsilon_l,\quad \alpha_h^2=\gamma^2+k_0^2\epsilon_h\ . \tag{6}$$

Next require $\hat{\mathbf{z}}\cdot\mathbf{H}$ and $\hat{\mathbf{x}}\cdot\mathbf{E}$ to be continuous across $y=t/2$, which will determine $A$ and the possible "eigenvalues" of $\gamma$. Using, from (2) and (3), $\hat{\mathbf{x}}\cdot\mathbf{E}=[i/k_0\epsilon(y)]\partial H/\partial y$, we obtain

$$\frac{\alpha_l}{\epsilon_l}\sin\frac{\alpha_l t}{2}\cos\alpha_h\left[\frac{a-t}{2}\right]+\frac{\alpha_h}{\epsilon_h}\cos\frac{\alpha_l t}{2}\sin\alpha_h\left[\frac{a-t}{2}\right]=0\ , \tag{7}$$

$$A=\frac{\cos(\alpha_l t/2)}{\cos\alpha_h[(a-t)/2]}\ . \tag{8}$$

Equations (6) and (7) require in general a numerical solution. For our parameter choices we usually have

$$|\epsilon_h|\gg|\epsilon_l\gg1\ , \tag{9}$$

which allows us to separate the solutions into two sets which are related to the simple results that hold in the extreme limit of (9). In this limit (7) may be approximated by

$$\sin\frac{\alpha_l t}{2}\cos\alpha_h\left[\frac{a-t}{2}\right]\approx0 \tag{10}$$

which is solved either by

$$\alpha_l(n)=2n\pi/t,\quad n=0,1,2,\ldots,\qquad A(n)=0 \tag{11}$$

or by

$$\hat{\alpha}_h(n)=(2n+1)\pi/(a-t),\quad n=0,1,2,\ldots,\qquad \hat{A}(n)=\infty\ . \tag{12}$$

We use here a caret over symbols that refer to the second set of solutions. Some typical results are shown in Fig. 2 for which $1/\sigma_h=10\ \Omega$, $1/\sigma_l=1000\ \Omega$, $\omega/2\pi c=\nu=80\ \mathrm{cm}^{-1}$, $a=0.872\ \mu\mathrm{m}$, $t/a=0.5$, and $D=0.001$ or $0.1\ \mu\mathrm{m}$. Solutions of the first set are large mostly in the low conducting region, while those of the second set are greatest in the highly conducting region. The approximations in (11) and (12) are seen to be useful guides (and first numerical guesses) to the exact solutions of (6)—(8). It is remarkable that in the perfectly conducting limit, $\sigma_h=\infty$, only the first set of solutions is relevant.

With the eigenfunctions known, we next expand the total field in terms of them. For simplicity we initially ignore the 2DEG and set $\epsilon_0=\epsilon_s$. Then we may write

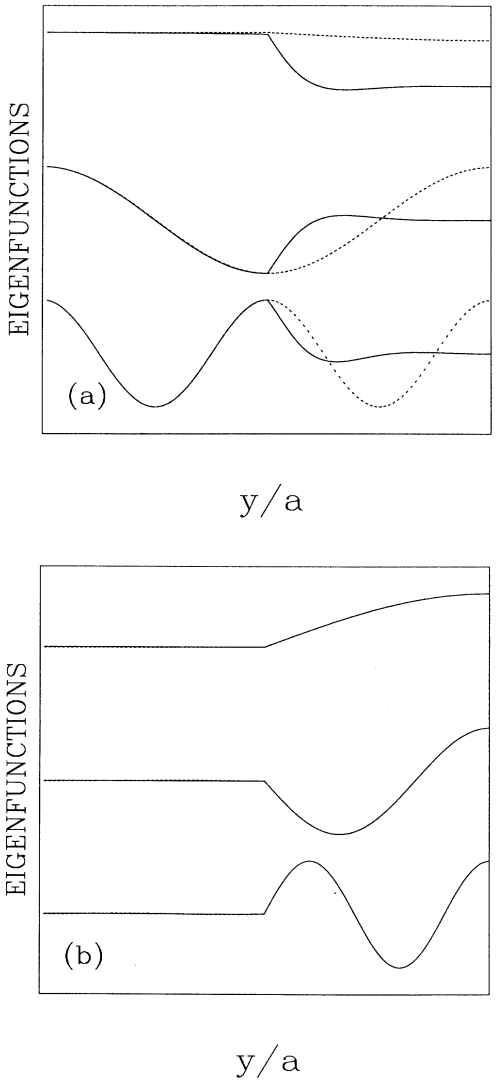


FIG. 2. Real part of the eigenfunctions of Maxwell's equations within the grating. The first three members of the two sets of solutions for $h(y)$ in (2) are shown, where (a) is for the first set, (b) is for the second set, and counting downward are $n=0,1,2$, respectively. Each $h(y)$ is normalized to unity at either $y=0$ or $y=a/2$. The middle of the $y$ axis at $y=t/2=a/4$ is the boundary between $\sigma_h$ and $\sigma_l$ regions. The solid curves have $D=0.001\ \mu\mathrm{m}$ and the dotted curves have $D=0.1\ \mu\mathrm{m}$. In (b) the results for the two values of $D$ are indistinguishable.

$$\hat{\mathbf{z}}\cdot\mathbf{H}_{\text{total}}(x,y)=\begin{cases} e^{ik_0(x+D)}+r_0e^{-ik_0(x+D)}+\sum_{n\geq 1} r_n e^{G_n^0(x+D)}\cos G_n y, & x\leq -D \\ \sum_{n\geq 0} h_n(y)(B_n^+ e^{\gamma_n x}+B_n^- e^{-\gamma_n(x+D)})+\sum_{n\geq 0}\hat{h}_n(y)(\hat{B}_n^+ e^{\hat{\gamma}_n x}+\hat{B}_n^- e^{-\hat{\gamma}_n(x+D)}), & -D\leq x\leq 0 \\ t_0 e^{ik_s x}+\sum_{n\geq 1} t_n e^{-G_n^s x}\cos G_n y, & 0\leq x\ , \end{cases} \tag{13}$$

where $k_0=\omega/c$, $k_s=\sqrt{\epsilon_s}k_0$, $G_n=2\pi n/a$, $G_n^0=(G_n^2-k_0^2)^{1/2}$, $G_n^s=(G_n^2-k_s^2)^{1/2}$. To determine the unknowns in the expansion we require continuity of $\hat{\mathbf{z}}\cdot\mathbf{H}$ and $\hat{\mathbf{y}}\cdot\mathbf{E}=(-i/k_0)(\partial/\partial x)\hat{\mathbf{z}}\cdot\mathbf{H}/\epsilon(y)$ across $x=-D$ and $x=0$. The various basis functions in the variable $y$ appearing in (13) leave some ambiguity about which to use in the matching process. We find that the numerical results can be quite unstable (in their dependence on the cutoff of the $n$ sums) if an inappropriate choice is made. Specifically, using $\cos G_n y$ everywhere gives trouble, while the following choice has yielded the most stable results.[9] With $\Delta$ denoting "the jump in the value of," we use across both $x=-D$ and $x=0$

$$\begin{aligned} &\Delta(\hat{\mathbf{y}}\cdot\mathbf{E})=0 \quad \text{along } 0\leq|y|\leq a/2, \quad \text{expanded in } \cos(2\pi n y/a)\ , \\ &\Delta(\hat{\mathbf{z}}\cdot\mathbf{H})=0 \quad \text{along } 0\leq|y|\leq t/2, \quad \text{expanded in } \cos(2\pi n y/t)\ , \\ &\Delta(\hat{\mathbf{z}}\cdot\mathbf{H})=0 \quad \text{along } 0\leq|y|-a/2|\leq(a-t)/2, \quad \text{expanded in } \cos[(2n+1)\pi(y-a/2)/(a-t)]\ . \end{aligned} \tag{14}$$

Since the form of the $h_n(y)$ and $\hat{h}(y)$ are known analytically, their expansion in terms of the various cosine functions in (14) is easy. We find converged results for $n_{\max}\sim 10$.

In Fig. 3 we show results for the transmission through the (isolated) grating: $T=|t_0|^2/\sqrt{\epsilon_s}$. The parameters are the same as in Fig. 2 except that we use three different $t/a$ values and plot versus $D$. The 2D approximation is also shown and works well out to $D\approx a$.

Finally consider the grating coupled to a 2DEG. We describe the latter by 2D free-electron equations using a simple Drude formula for the layer's conductance. We ignore effects of the finite thickness, corrugation, static $\mathbf{B}\neq 0$, etc., since our focus is on the strength of local fields produced by the grating in the vicinity of the 2DEG. We find the net transmission through the system by a multiple scattering scheme in which the electromagnetic waves

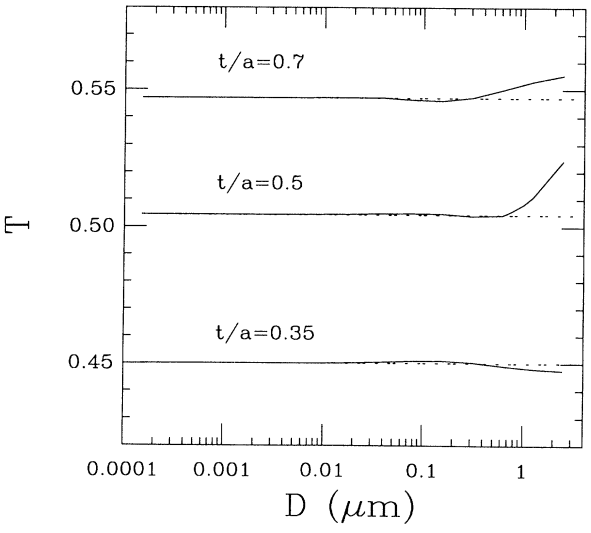


FIG. 3. Transmission coefficient of isolated 3D and 2D grating with a common conductance profile. The grating parameters are the same as Fig. 2 except for the $t/a$ ratios and $\epsilon_0=\epsilon_s=12.8$. The 3D results (solid curves) do not significantly deviate from the 2D approximations (dotted lines) until $D$ exceeds $a$.

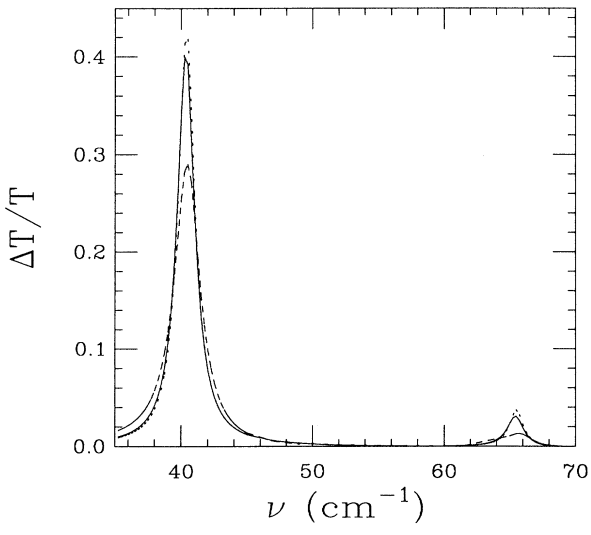


FIG. 4. Frequency dependence of the fractional change in transmission (with and without the 2DEG) calculated from Eq. (15). The solid curve is for $D=0.1a=0.0872$ $\mu$m, the dashed curve for $D=0.5a=0.436$ $\mu$m. The 2D result is the dotted curve. For $D<0.1a$ the 3D curve almost overlaps the 2D curve. The 2DEG has a carrier density of $6.7\times10^{11}/\text{cm}^2$, an effective mass 0.071 that of a free electron, and a Drude scattering time of 4.5 psec. See text for other parameter values.

bounce back and forth between the grating and the 2DEG. Indeed the optical problem has the same formal appearance as that for the transmission of a beam through two parallel interfaces. The required inputs are simply the reflection and transmission amplitudes of each "interface"; i.e., of the grating and of the 2DEG. Skipping over the straightforward derivation, we note that the net transmission amplitude can be written as

$$t^{\text{net}} = \sum_G t^{(g)}_{0G}(1 - \mathbf{P}\cdot\mathbf{r}^{(s)}\cdot\mathbf{P}\cdot\mathbf{r}^{(g)})^{-1}_{G0} P_{00} t^{(s)}_{00} , \quad (15)$$

where the various factors are matrices indexed by reciprocal lattice vectors (along $\hat{\mathbf{y}}$). The only nondiagonal matrices are those that refer to the grating (with a superscript $g$) and describe either reflection off or transmission through it. The analogous quantities with an $s$ superscript describe the 2DEG system and, like the propagation amplitude $\mathbf{P}$ for motion between the grating and 2DEG, are diagonal matrices since they do not involve diffraction.

Results calculated from (15) with $t/a = 0.35$ are shown in Fig. 4, using parameters for the 2DEG from Ref. 3 and grating parameters from Fig. 2. The same qualitative conclusion holds as for Fig. 3, except that the deviation between 3D and 2D solutions becomes more quickly evident as $D$ increases. This is easy to rationalize since any diffracted fields, which alone are responsible for the resonances seen in Fig. 4, decay along the $x$ axis and hence are sensitive to finite thickness effects. Note that, consistent with this argument, the higher-order plasmon absorption peak is more noticeably distorted.

To summarize, we have derived and evaluated expressions for the electromagnetic coupling between a 3D grating and a nearby 2DEG. Examination of the influence of the thickness of the grating justifies our earlier 2D treatment as a limiting case and allows a quantitative treatment of the deviations that can develop.

This work was supported in part by the NSF through Grant No. DMR 89-03851.

[1]S. J. Allen, Jr., D. C. Tsui, and R. A. Logan, Phys. Rev. Lett. **38**, 980 (1977).
[2]T. N. Theis, J. P. Kotthaus, and P. J. Stiles, Solid State Commun. **24**, 273 (1977).
[3]E. Batke, D. Heitmann, and C. W. Tu, Phys. Rev. B **34**, 6951 (1982).
[4]L. Zheng, W. L. Schaich, and A. H. MacDonald, Phys. Rev. B **41**, 8493 (1990).
[5]R. Petit and G. Tayeb, J. Opt. Soc. Am. A **7**, 1686 (1990).
[6]*Electromagnetic Theory of Gratings,* edited by R. Petit (Springer, New York, 1980).
[7]There is a collection of articles on grating diffraction in J. Opt. Soc. Am. A **7** (8 and 9) (1990).
[8]Ping Sheng, R. S. Stepleman, and P. N. Sanda, Phys. Rev. B **26**, 2907 (1982).
[9]We find instabilities if $D$ goes below 1 Å.